Asian Journal of Chemistry; Vol. 38, No. 8 (2026), 1995-2004
ASIAN JOURNAL OF CHEMISTRY
https://doi.org/10.14233/ajchem.2026.36118

Application of *Azolla pinnata* Biochar as a Green Low-Cost Solid Catalyst in the Production of Biodiesel from Tamarind Kernel Oil

BANDANA SINGHA[1] and DIBAKAR CHANDRA DEKA[2,*]

[1]Department of Chemistry, Gauhati University, Guwahati-781001, India
[2]Department of Chemistry, Mizoram University, Aizawl-796004, India

Corresponding author: E-mail: dcdeka@gauhati.ac.in; dcdeka@rediffmail.com

Received: 1 April 2026 *Accepted*: 5 June 2026 *Published online*: 7 August 2026 AJC-22425

This work reports a heterogeneous base catalyst obtained from the waste biomass *Azolla pinnata* as an effective catalyst in the transesterification of tamarind kernel oil (TKO) for biodiesel generation. The biochar catalyst was generated by pyrolysis of the ash obtained from burning the dry *A. pinnata* waste at 500 ºC for 3 h and characterised before and after use using instrumental techniques like powder XRD, FESEM, EDX, BET and TGA analysis. The main components of the catalyst are KCl, NaCl and SiO_2 along with significant amounts of MgO, CaO and $CaCO_3$. The TKO was extracted from tamarind seeds using different solvents out of which, *n*-hexane was found to be the best with an average oil yield of 19.3% in 5 h. The catalyst demonstrated remarkable catalytic efficacy in transforming tamarind kernel oil into biodiesel, achieving a 98% yield at ambient temperature under optimal circumstances of 10:1 methanol-to-oil ratio and 20 wt.% catalyst over a reaction period of 3 h. The catalyst was used up to the third consecutive cycle of the reaction with only minimal loss in catalytic activity. The catalyst is eco-friendly, non-toxic, biodegradable, recoverable, reusable and cost-effective.

Keywords: *Azolla pinnata*, Biochar, Biocatalyst, Biodiesel, Biowaste.

INTRODUCTION

Depleting fossil fuel reserves and environmental pollution are the two major threats that the planet earth is currently facing due to the over-exploitation of the limited resources by the ever-growing population which is estimated to reach 9 billion by 2050. There is an urgent need that we rediscover all polluting chemical processes to minimize environmental pollution caused due to chemical industries and to reduce our dependency on petroleum fuels as well. The current demand of annual worldwide primary energy consumption is 12 billion tons [1] out of which 77% of this demand is met by fossil fuels [2]. The United Nations Member States in 2015 adopted 17 Sustainable Development Goals (SDGs) as part of the 2030 Agenda for Sustainable Development out of which one is to substantially increase the share of renewable energy in the global energy mix by 2030. Hence to achieve this target, the search for cleaner alternative fuels and production technology needs to be substantially increased.

Biodiesel is a renewable, environmentally friendly alternative to petroleum diesel that can be directly used in conventional diesel engines. It is primarily produced by transesterification of vegetable oils and animal fats. Based on feedstock and production technology, biofuels are classified into four generations. First-generation biodiesel is produced from edible oils such as palm, sunflower and soybean, but its reliance on food crops has led to the food *versus* fuel debate. Second-generation biofuels, derived from non-edible biomass, lignocellulosic feedstocks and municipal wastes, overcome these limitations while contributing to waste management. Third-generation biofuels are produced from algae, which have oil yields 15-300 times higher than conventional crops, although economic feasibility remains a challenge. Fourth-generation biofuels, derived from genetically modified algae, are still in the early stages of development [3].

Among second-generation feedstocks, non-edible oils from *Calophyllum inophyllum*, *Pongamia pinnata*, *Jatropha curcas*, *Croton megalocarpus* and *Thevetia peruviana* have been widely investigated for biodiesel production. However, tamarind seed oil remains largely underutilised. Tamarind (*Tamarindus indica* Linn.) is a drought-tolerant, nitrogen-fixing tree capable of growing in poor soils with minimal agricultural inputs. Its

seeds, constituting nearly 34% of the fruit, are generated in large quantities as byproducts of the tamarind pulp industry and are mostly discarded despite their considerable oil content [4]. Their abundance and low cost make them an attractive sustainable feedstock for biodiesel production.

Among the available biodiesel production methods, transesterification is the simplest and most economical. In this process, triglycerides react with methanol in the presence of a catalyst to produce fatty acid methyl esters (biodiesel) and glycerol. Catalysts used for transesterification include synthetic catalysts [5], biomass-based catalysts [6], carbon-based catalysts and enzyme-based catalysts [7]. However, synthetic catalysts are expensive and environmentally unfavourable. Consequently, heterogeneous catalysts derived from waste biomass have attracted increasing attention since they are inexpensive, sustainable and help mitigate solid waste disposal problems. Biomass-derived catalysts prepared from waste eggshells [5], oyster shells [6] and other waste materials have demonstrated excellent catalytic activity in biodiesel production and other organic transformations. Likewise, rapidly growing aquatic weeds such as *Eichhornia*, *Azolla* and *Lemna*, which proliferate in lakes and wetlands, represent abundant renewable sources for catalyst preparation [7].

Azolla is a fast-growing aquatic fern that thrives in stagnant water bodies and can double its biomass within two days through its symbiotic association with *Anabaena azollae*. Among its six extant species, *Azolla pinnata* is widely distributed across Asia, including the Indian subcontinent and possesses enormous biomass potential. The development of heterogeneous catalysts from such invasive biomass is of considerable significance due to their rapid growth, easy availability and minimal cost. To date, *A. pinnata* has not been extensively explored as a precursor for heterogeneous catalysts in biodiesel production. Therefore, in the present study, a biochar-based heterogeneous catalyst derived from waste *A. pinnata* biomass was successfully employed for the transesterification of tamarind seed oil to biodiesel (fatty acid methyl ester). The effects of catalyst loading, methanol-to-oil ratio, catalyst reusability, leaching behaviour and catalyst characterisation before and after use were systematically investigated and compared with previously reported waste biomass-derived catalysts. The developed catalyst exhibited excellent catalytic performance, highlighting its potential as a low-cost and sustainable catalyst for biodiesel production.

EXPERIMENTAL

The tamarind seed pods were collected from the trees available in plenty in villages of Assam state, India. *Azolla pinnata* is abundantly available throughout Northeast India. It is found as a free-floating water fern in various lakes and ponds. Samples were collected from the freshwater lake Deepor beel, located at 26.13ºN, 91.66ºE, India. Solvents and other chemicals used were of analytical grade and were collected from commercial sources and used as such unless stated otherwise.

Preparation of catalyst: The *A. pinnata* biomass was washed several times with fresh water to remove any unwanted impurities followed by drying in open air for a few days during which 3 kg of wet raw mass was reduced to 250 g of dry mass. Dry material (250 g) was slowly burned in an earthen tray to yield 31 g of ash (APA-C0). The ash was then calcined for 3 h at 500 ºC in a programmed muffle furnace to yield the biochar. After the heating process was finished, the biochar was kept in a desiccator to cool it to room temperature and stored there until use. The *A. pinnata* biochar catalyst is named as APA-C500.

Characterisation: Powder X-ray diffraction (XRD) was used to evaluate the chemical composition of the *A. pinnata* ash using a Rigaku, Ultima-IV powder X-ray diffractometer using Cu-*K*α as the X-ray source (λ = 1.546 Å), a 2θ scan spanning the range of 10-80º, with a step size of 0.02º and a scan rate of 2º/min. FESEM image and EDX of the sample were obtained from Oxford liquid nitrogen free SDD X MAX 50 EDS. Prior to examination, the sample was coated with gold. FESEM, Supra 55, Carl Zeiss, Germany, offered precise imaging information regarding the morphology and surface texture of the sample. ^{1}H NMR spectra were recorded using Bruker DPX-300 MHz spectrometer. $CDCl_3$ was used as the solvent and chemical shifts were recorded relative to $SiMe_4$, as the internal reference. BET Micromeritics Tristar 3000 equipment was used to measure the sample's surface area, pore volume and pore size. Adsorption of N_2 adsorption-desorption isotherms at 77 K was used to calculate the specific surface area using the Brunauer-Emmett-Teller (BET) formula. Data on N_2 adsorption were collected over the vapour pressure range (P/Po) of 0.05 to 0.3. The samples were degassed for 3 h at 50-250 ºC in a He atmosphere before being subjected to N_2 adsorption analysis. The Barrett-Joyner-Halenda (BJH) technique was used to determine pore size distributions from desorption isotherms. To evaluate the heat stability of the sample and to determine the calcination temperature for the catalyst, thermogravimetric analysis (TGA) was employed. The TGA spectra of the uncalcined *A. pinnata* biochar APA-C0 sample were obtained using the TGA/DSC-1, METTLER TOLEDO, from ambient temperature to 700 ºC at a scanning rate of 10 ºC/min in a nitrogen environment.

Tamarind kernel powder (TKP) preparation: Tamarind seeds were manually separated from the pulp, inspected to remove damaged or pest-infested seeds and thoroughly washed to eliminate adhering pulp. To facilitate removal of the hard seed coat (testa), the seeds were soaked in water at room temperature for three days. The softened seed coats were manually removed, and the kernels were washed and air dried for 1-2 days to remove moisture. The dried kernels were pulverised into fine tamarind kernel powder (TKP), which was further sun-dried for 30 min to obtain a clean white powder. To prevent moisture absorption and spoilage during storage, the TKP was sealed in airtight containers and stored in a desiccator.

Tamarind kernel oil (TKO) extraction: TKP (10 g) was lightly roasted in an oven for 15 min before solvent extraction. The powder was extracted with 100 mL of solvent (10 mL/g) by magnetic stirring for 3 h at room temperature. The extract was filtered and the residue was re-extracted twice with fresh solvent to maximize oil recovery. The combined filtrates were dried over anhydrous Na_2SO_4 and the solvent was removed under reduced pressure using a rotary evaporator followed by high vacuum to obtain crude tamarind seed oil.

n-Hexane, petroleum ether (bp 40-60 ºC) and diethyl ether were evaluated as extraction solvents, with *n*-hexane providing the highest oil yield. The crude oil was characterized by NMR and further purified by column chromatography using ethyl acetate/petroleum ether (1:20, v/v) as the eluent.

Transesterification of tamarind seed oil to fatty acid methyl ester (FAME) using APA catalyst: Transesterification of TKO to biodiesel (fatty acid methyl ester) was done using methanol as solvent in the presence of catalyst derived from *A. pinnata* at room temperature (30-32 ºC) with 20 wt.% of catalyst to afford around 98% of yields. A mixture of the oil, methanol (10 mL/g oil) and the catalyst (20 wt.% of oil) stirred magnetically in a round bottom flask at room temperature. The progress of the reaction mixture was monitored by TLC. After the reaction was completed, the catalyst was removed by filtration. The mixture of crude product and glycerol was allowed to stand in a separating funnel. After few hours, two separate layers are formed. The bottom layer consists of the glycerol as it was insoluble in the esters and had a much higher density and the top layer consists of the FAME from TKO. The glycerol layer was separated and the crude FAME was collected, concentrated under reduced pressure and purified by silica gel column chromatography using ethyl acetate/petroleum ether (1:20, v/v) as eluent.

Reusability of catalyst: To evaluate catalyst reusability, successive transesterification reactions were performed under the optimised conditions. After each cycle, the catalyst was recovered by filtration, washed thoroughly with methanol followed by petroleum ether, dried at 110-120 ºC for 2-3 h, and reactivated by calcination at 350 ºC for 1 h in a muffle furnace. The regenerated catalyst was cooled in a desiccator and reused. The fresh and reused catalysts were characterised by FESEM, EDX and PXRD.

RESULTS AND DISCUSSION

PXRD analysis: The PXRD patterns of the uncalcined (APA-C0) and calcined (APA-C500) *A. pinnata* biochar catalysts are shown in Fig. 1, respectively. Both patterns exhibit well-defined diffraction peaks confirmed the presence of crystalline phases. The PXRD profile of APA-C0 confirms the presence of nanocrystalline mineral phases, consistent with the FESEM observations. Phase identification was performed by matching the observed 2θ values with JCPDS database entries and previously reported literature.

Potassium was identified as the predominant inorganic constituent, occurring mainly as KCl (sylvite). The intense reflections at 2θ = 28.34º and 40.52º, together with peaks at 50.19º, 58.81º, 66.39º and 73.71º (JCPDS card No. 41-1476), confirm the presence of crystalline KCl, indicating a high potassium content in the biochar. Similar diffraction features have been reported for coconut husk ash-derived biochar by Vadery *et al*. [8]. Sodium chloride (halite) was also identified in APA-C0 at 2θ = 27.18º, 31.62º, 45.40º, 56.42º and 75.19º (JCPDS card No. 00-05-0628). Crystalline SiO_2 (quartz) was confirmed by the characteristic peaks at 2θ = 20.85º and 26.64º (JCPDS card No. 01-083-0539), in agreement with the straw slag catalyst reported by Wang *et al*. [9].

Calcination at 500 ºC resulted in significant mineralogical transformations. A new crystalline SiO_2 (cristobalite) phase appeared, as evidenced by reflections at 2θ = 22.2º, 28.7º, 31.8º and 36.4º (JCPDS card No. 00-039-1425). The presence of $CaCO_3$ (calcite) was confirmed by diffraction peaks at 2θ = 29.3º, 36.0º, 39.4º, 47.3º and 48.4º (JCPDS card No. 05-0586), consistent with the freshwater mussel shell catalyst reported by Hu *et al*. [10]. Partial thermal decomposition of $CaCO_3$ during calcination produced CaO, identified by reflections at 2θ = 32.2º, 37.6º and 54.2º. Additional crystalline phases detected after calcination included $SiCl_4$ (2θ = 31.6º, 40.4º, 45.4º and 49.9º), MgO (2θ = 42.9º, 62.3º and 78.6º; JCPDS card No. 87-0653) and trace amounts of aphthitalite, $K_3Na(SO_4)_2$ (2θ = 30.3º, 31.48º and 44.3º; JCPDS card No. 00-20-0928).

The PXRD patterns of the regenerated catalysts after the second (APA-CAU) and third (APA-CAU1) reuse cycles are shown in Fig. 2. Compared with APA-C500, the diffraction peaks corresponding to KCl, NaCl, $SiCl_4$, CaO and MgO disappeared after reuse, whereas new reflections corresponding to $MgSiO_3$ appeared after the second cycle and $KMg(PO_3)_3$ after the third cycle, likely as a consequence of recalcination at 350 ºC during catalyst regeneration. In contrast, the diffrac-

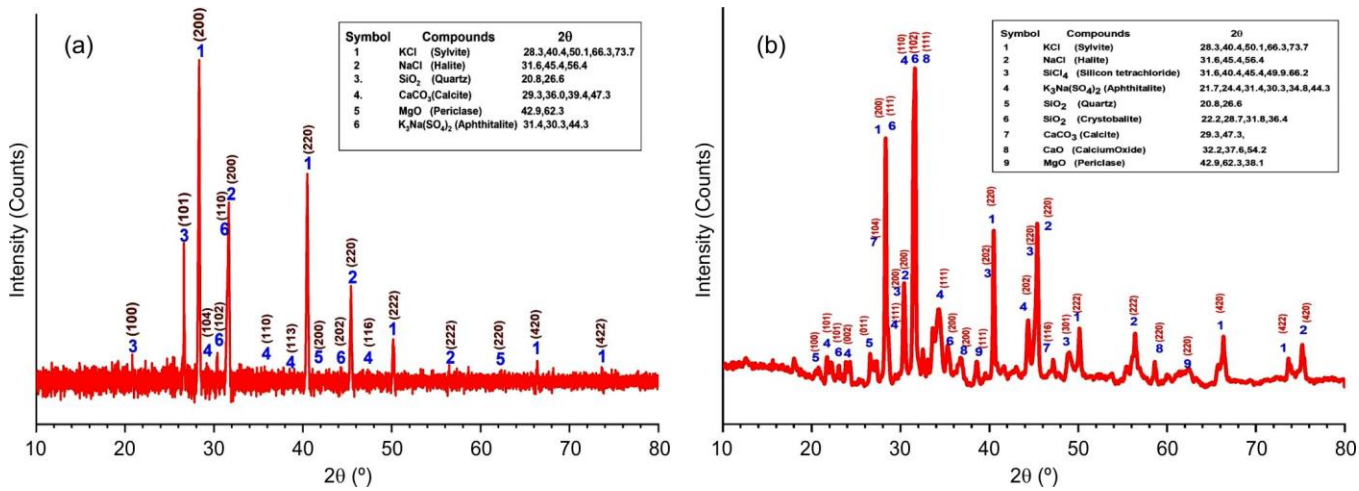

Fig. 1. PXRD of (a) uncalcined catalyst (APA-C0) and (b) calcined catalyst (APA-C500)

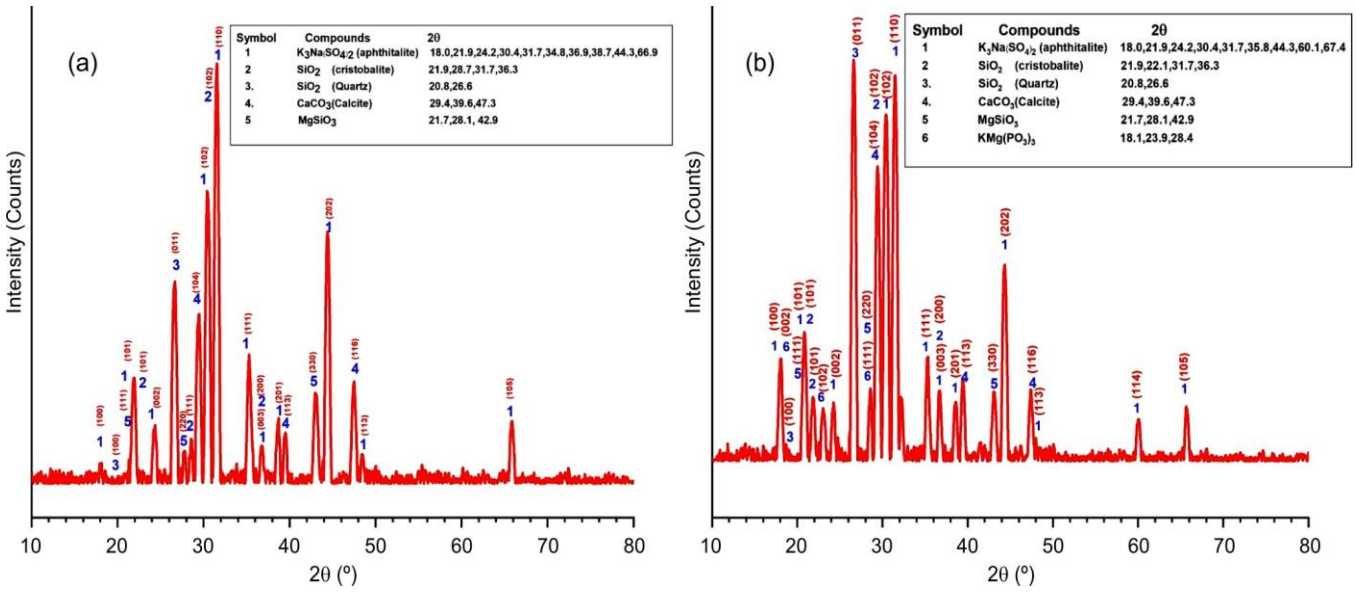

Fig. 2. PXRD of (a) catalyst after 2nd cycle (APA-CAU) and (b) catalyst after 3rd cycle (APA-CAU1)

tion peaks of SiO_2 and $CaCO_3$ remained essentially unchanged, and both phases retained their structural integrity during repeated catalytic cycles. The disappearance of K-, Cl-, Ca- and Mg-containing phases after reuse suggests that these species constitute the catalytically active components and undergo transformation or leaching during transesterification. The EDX results (Table-1) showed a pronounced decrease in chloride content, from 19.48 wt.% in the fresh catalyst to 0.25 wt.% after reuse, attributable to the loss of chloride-containing species during catalytic operation.

TABLE-1
ELEMENTAL COMPOSITION (wt.%) OF *Azolla pinatta* CATALYST BEFORE USE (APA-C500) AND AFTER 2nd USE (APA-CAU) AND 3rd REUSE (APA-CAU1)

Catalyst	Elements content (wt.%)		
	Na	K	Cl
APA-C500	9.75	20.12	19.48
APA-CAU	6.32	8.54	0.25
APA-CAU1	5.74	7.31	0.24

EDX analysis: The EDX spectra of the calcined *A. pinnata* biochar catalyst (APA-C500) before transesterification and after the first (AU-1st), second (AU-2nd) and third (AU-3rd) reuse cycles are shown in Fig. 3. The fresh catalyst primarily comprised C, O, Si, Na, Mg, Ca, K and Cl, while P, S, Fe, Mn, Al and N were detected in trace amounts. These results are consistent with the PXRD analysis. After repeated use, the intensities of the Na, K, Ca and Cl peaks decreased markedly confirmed the participation of these species in the catalytic process. As shown in Table-1, the wt.% of Na, K and Cl decreased from 9.75, 20.12 and 19.48 in the fresh catalyst to 6.32, 8.54 and 0.25, respectively, after reuse, suggesting partial leaching or transformation of the active inorganic species during transesterification.

FESEM analysis: The surface morphology and microstructure of the catalysts were investigated by FESEM. Representative micrographs of the calcined *A. pinnata* biochar catalyst (APA-C500) before use and after the first (AU-1st), second (AU-2nd) and third (AU-3rd) reuse cycles are shown in Fig. 4. The uncalcined biochar (APA-C0, not shown) exhibited a relatively compact, non-porous and irregular surface with dispersed nanostructured particles. Calcination at 500 ºC markedly altered the morphology, producing well-defined polycrystalline structures with increased crystallinity. The surface transformed from relatively smooth and compact to one consisting of agglomerated crystalline particles with enhanced surface roughness, which contributed to an increase in BET surface area from 8 to 11 m^2/g and is expected to improve catalytic performance.

The calcined catalyst contained agglomerates of irregularly shaped nanoparticles, including rhombohedral (159-372 nm), hexagonal (152-257 nm), sheet- or needle-like (~370 nm) and spherical particles (12-52 nm). These crystalline features became more distinct after calcination confirmed the formation of catalytically active mineral phases.

Following repeated transesterification cycles, progressive agglomeration of nanoparticles and a gradual reduction in surface roughness were observed. After the first reuse, most of the hexagonal, cylindrical and sheet-like particles became smoother and partially distorted, although localised crystalline regions remained. The characteristic hexagonal particles decreased in size from approximately 5.5 μm to about 800 nm in length and from 487-524 nm to 185-252 nm in width, indicating structural reconstruction during catalyst regeneration and use. Despite these morphological changes, appreciable crystallinity persisted after repeated cycles, supporting the observed catalyst reusability. After the third reuse cycle, newly formed spherical particles with diameters of 322-639 nm were observed, which were absent in the fresh catalyst, suggesting phase transformation and particle sintering during repeated calcination and catalytic operation. The FESEM results indicate that although repeated use causes particle agglomeration and surface smoothing, the catalyst retains its crystalline structure, which contributes to its sustained catalytic activity over successive reaction cycles.

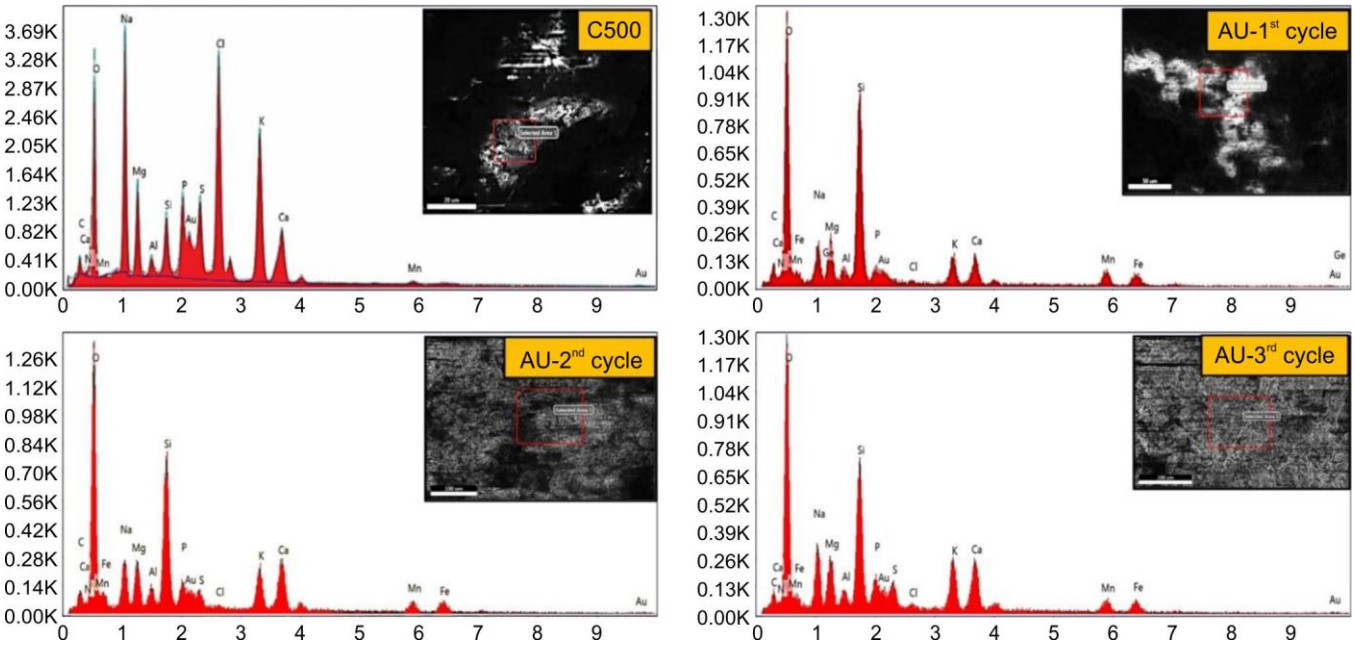

Fig. 3. EDX of the catalyst before use (C500) and after use (AU-1st cycle), (AU-2nd cycle) and (AU-3rd cycle) and after use

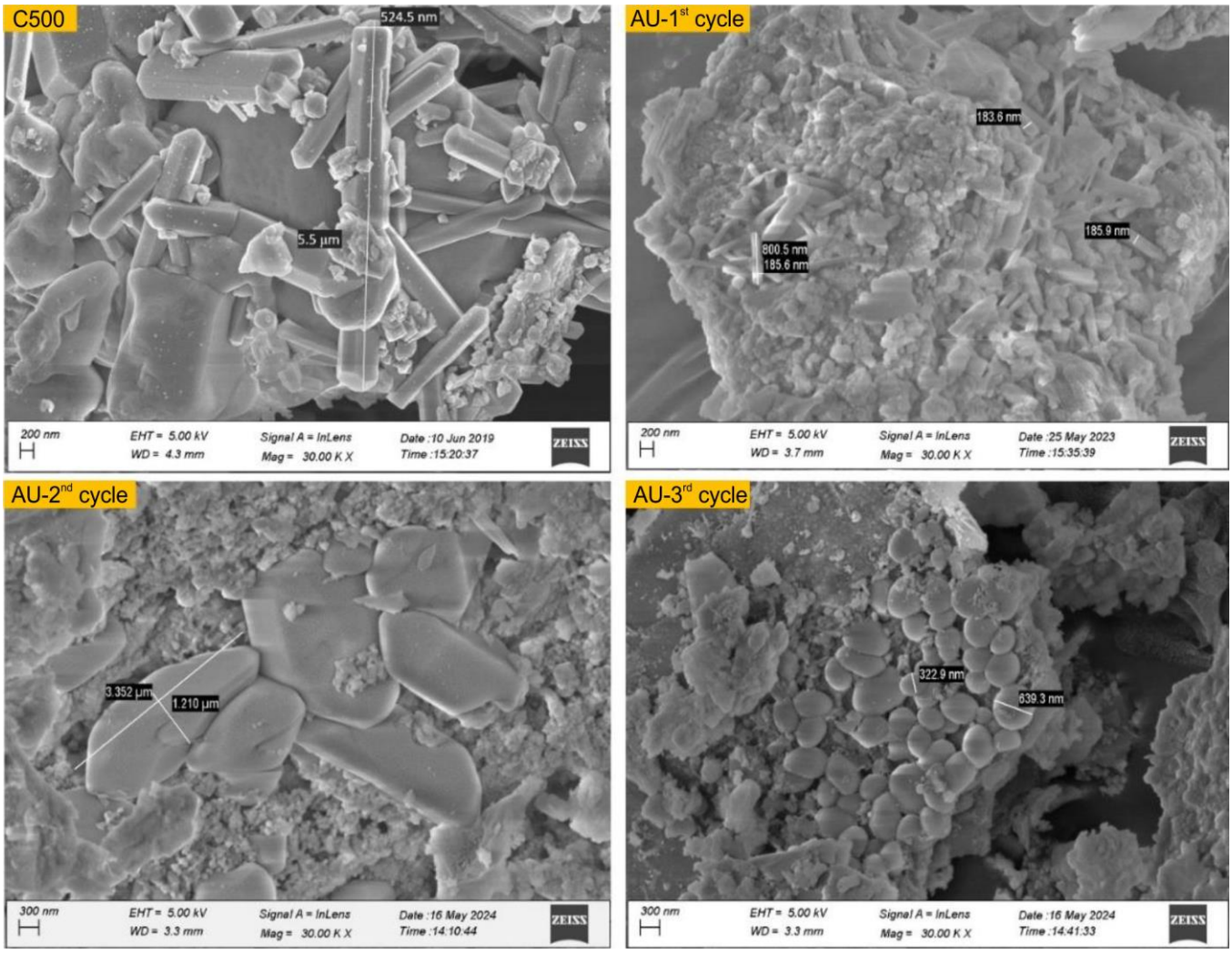

Fig. 4. FESEM of the catalyst before use (C500) and after use (AU-1st cycle), (AU-2nd cycle) and (AU- 3rd cycle)

BET surface area, pore volume and pore size: The BET surface area of the uncalcined *A. pinnata* biochar (APA-C0) was 8 m^2/g, with a micropore volume of 0.0077 8 cm^3/g and an average mesopore diameter of 16.2 nm. Calcination at 500 ºC increased the surface area to 11 m^2/g representing a 31.7% increase following pyrolysis. This enhancement is attributed to the development of additional porous structures during thermal activation.

The surface area of APA-C500 is comparable to those of several biomass-derived heterogeneous catalysts reported for biodiesel production, including calcined quail eggshells (14 m^2/g) [11], waste mud crab shell (13 m^2/g) [12], and exceeds that of waste obtuse horn shell-derived CaO (0.07 m^2/g) [13], all of which have demonstrated excellent transesterification performance. The increase in surface area upon calcination provides more accessible active sites, thereby facilitating transesterification and enhancing FAME production consistent with previous reports [14]. These findings demonstrate that *A. pinnata* biochar is a promising low-cost biomass-derived heterogeneous catalyst for biodiesel synthesis.

Thermal analysis: Thermogravimetric analysis (TGA) of the uncalcined *A. pinnata* biochar (APA-C0) was performed from room temperature to 700 ºC at a heating rate of 10 ºC/min under a nitrogen atmosphere to evaluate its thermal stability. The TGA profile (not shown) exhibited three distinct stages of weight loss. The biomass remained thermally stable up to approximately 500 ºC, beyond which rapid mass loss occurred due to the decomposition of carbonate species. Based on the TGA results, 500 ºC was selected as the optimum calcination temperature for catalyst preparation.

Solvent selection and optimisation of extraction time: The extraction efficiency of tamarind kernel oil using petroleum ether, *n*-hexane and diethyl ether was evaluated and the results are shown in Table-2. Among the solvents tested, *n*-hexane provided the highest oil yield (19.3%), followed by petroleum ether (16.8%) and diethyl ether (12.4%). Therefore, *n*-hexane was selected as the extraction solvent for all subsequent experiments. Complete oil extraction was achieved after 5 h of stirring using a solvent-to-kernel ratio of 10 mL/g consistent with the procedure reported for similar seed oils [15].

Catalytic activity in the transesterification of tamarind kernel oil to biodiesel

Effect of oil to catalyst ratio and reaction time: The transesterification reaction is influenced by several parameters including alcohol-to-oil molar ratio, catalyst loading, reaction temperature and reaction time. Among the commonly used alcohols, methanol was selected due to its low cost, high reactivity and good miscibility with the reaction medium. A series of reactions was conducted at room temperature (32 ºC) to optimize catalyst loading and reaction time.

Increasing the catalyst loading significantly enhanced biodiesel yield. Using 1 wt.% catalyst, a maximum yield of 46% was obtained after 3 h. Increasing the catalyst loading to 5, 10 and 20 wt.% improved the yield to 76%, 92% and 98%, respectively (Fig. 5), indicating that higher catalyst loading provides more accessible active sites for transesterification. Reaction time also influenced biodiesel production, with equilibrium being reached after approximately 2 h (Table-3). Further extending the reaction time produced no significant improvement in biodiesel yield, indicating completion of the reaction.

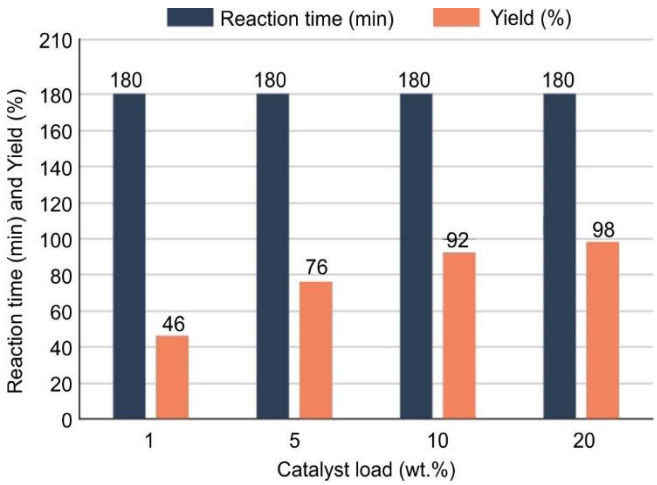

Fig. 5. Effect of catalyst loading (wt.%) on biodiesel yield. Reaction conditions: oil to methanol molar ratio = 1:10, reaction temperature = 32 ºC and reaction time = 180 min

Effect of oil to methanol ratio: The effect of the oil-to-methanol ratio on biodiesel production was investigated by varying the ratio from 1:2 to 1:20 (w/v). As shown in Fig. 6, the biodiesel yield increased from 42% to 98% with increasing methanol content, reaching a maximum at an oil-to-methanol ratio of 1:10. At lower methanol concentrations, the yield was limited because insufficient methanol failed to shift the transesterification equilibrium towards product

TABLE-2
EXTRACTABILITY OF SEED OIL USING VARIOUS SOLVENTS AT AMBIENT TEMPERATURE (30-35 ºC)

Solvent (10 mL/g of seed kernel)	Weight of kernel (g)	Stirring time (h)	Weight of crude oil (g)	Yield (crude oil) (wt.%)	Average yield (crude oil) (wt.%)
n-Hexane	10.05	3	1.88	18.8	19.3
	10.05	4	1.94	19.4	
	10.05	5	1.99	19.9	
Petroleum ether	10.05	3	1.64	16.4	16.8
	10.05	4	1.69	16.9	
	10.05	5	1.72	17.2	
Diethyl ether	10.05	3	1.22	12.2	12.4
	10.05	4	1.23	12.3	
	10.05	5	1.27	12.7	

TABLE-3
EFFECT OF OIL TO CATALYST (APA-C500) RATIO FOR THE TRANSESTERIFICATION OF THE SEED OIL TO BIODIESEL AT CONSTANT OIL TO SOLVENT RATIO (REACTION TEMPERATURE = 32 ºC)

Oil:methanol (w/v)	Oil:catalyst (w/w)	Time (h)	Yield (g)	Yield of biodiesel (wt.%)
1:10	100:1	1	0.22	22
		2	0.45	45
		3	0.46	46
		4	0.46	46
1:10	100:5	1	0.53	53
		2	0.75	75
		3	0.76	76
		4	0.77	77
1:10	100:10	1	0.90	90
		2	0.92	92
		3	0.92	92
		4	0.92	92
1:10	100:20	1	0.95	95
		2	0.97	97
		3	0.98	98
		4	0.98	98

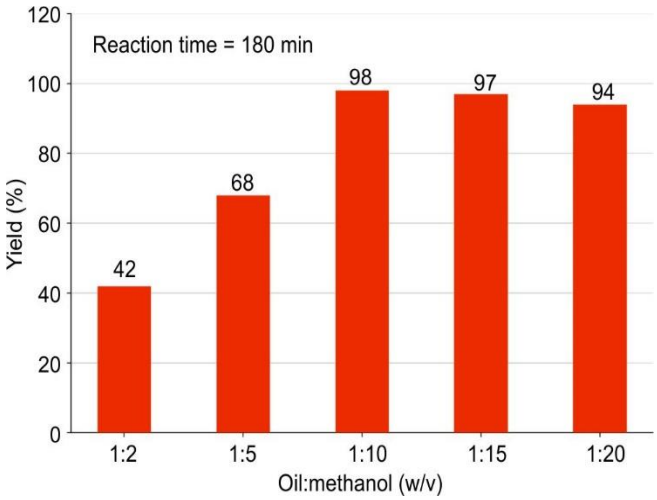

Fig. 6. Effect of oil to methanol ratio on biodiesel yield. Reaction conditions: catalyst loading = 20 wt.%, reaction temperature = 32 ºC and reaction time = 180 min

formation. Increasing the methanol content beyond 1:10 did not improve the conversion; instead, the yield decreased slightly to 94% at a ratio of 1:20. This reduction is attributed to the reversible nature of the base-catalysed transesterification reaction, where excess methanol promotes the formation of mono- and diglycerides [16] and increases glycerol solubility, thereby hindering catalyst-reactant interactions and reducing biodiesel conversion [13]. Thus, an oil-to-methanol ratio of 1:10 was identified as the optimum for maximum biodiesel yield.

NMR spectral analysis of TKO and FAME: The ^{1}H NMR spectra of tamarind kernel oil and the corresponding fatty acid methyl ester (FAME) are shown in Fig. 7, respectively. In the spectrum of tamarind kernel oil, the multiplet at δ 5.2-5.4 ppm corresponds to the olefinic protons of the unsaturated fatty acid chains, while the signals at δ 4.13, 4.29 and 5.29 ppm are assigned to the methylene and methine protons of the glycerol backbone in triglycerides. Following transesterification, these glycerol-associated signals disappeared and a characteristic singlet at δ 3.28 ppm, corresponding to the methoxy protons of the methyl ester, appeared in the FAME spectrum. These spectral changes confirm the successful conversion of tamarind kernel oil into biodiesel.

Reusability studies: The reusability of the *A. pinnata* biochar catalyst was evaluated by performing successive transesterification reactions under the optimised conditions. After each cycle, the catalyst was recovered, regenerated by washing and calcination at 350 ºC and reused. As shown in Table-4, the fresh catalyst produced 98.0% biodiesel yield in 3 h. Upon the first reuse, the yield decreased slightly to 94.8% in 3 h, but increased to 96.6% when the reaction time was extended to 5 h. During the second reuse (third reaction cycle), the catalyst afforded 91.1% yield in 3 h, which improved to 94.2% after 5 h.

Thus, the catalyst retained high catalytic activity after three consecutive cycles, with only a modest decline in biodiesel yield from 98.0% to 94.2% (Fig. 8). The gradual loss in activity is likely due to partial leaching of catalytically active species [16] and deposition of glycerol or methyl ester on the catalyst surface, which blocks active sites during repeated use [16]. Similar behaviour has been reported for other biomass-

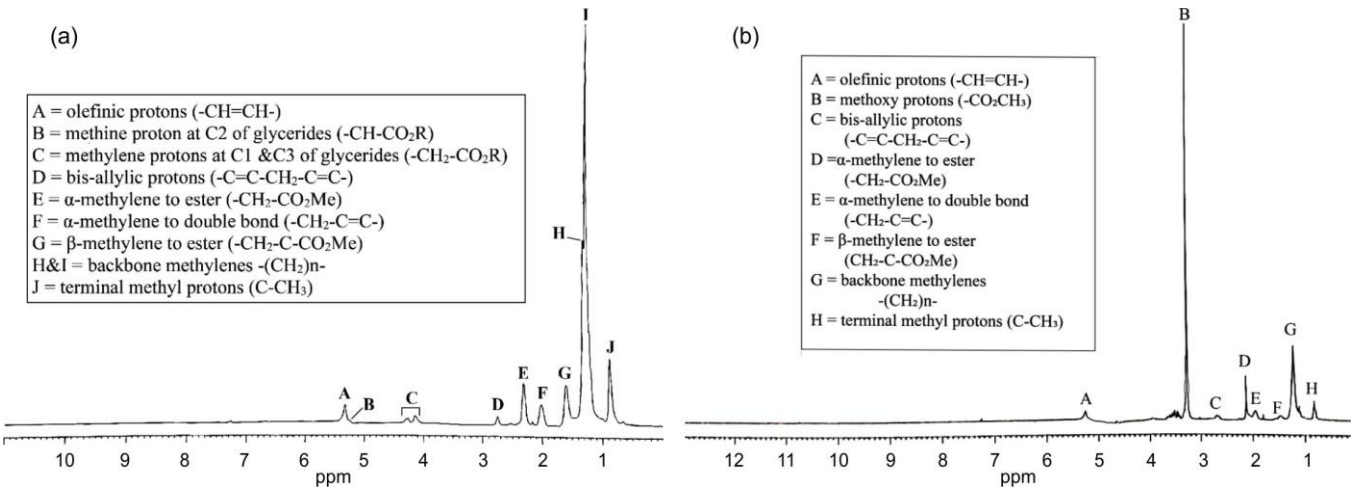

Fig. 7. ^{1}H NMR spectra of (a) tamarind kernel oil and (b) tamarind kernel methyl ester

TABLE-4
2nd CYCLE OF THE CATALYST
(APA-CAU) FOR TRANSESTERIFICATION

Oil:methanol (w/v)	Oil:catalyst (w/w)	Time (h)	Yield (g)	Biodiesel yield (wt.%)
1:10	100:20	1	0.933	93.3
		2	0.946	94.6
		3	0.948	94.8
		4	0.952	95.2
		5	0.966	96.6

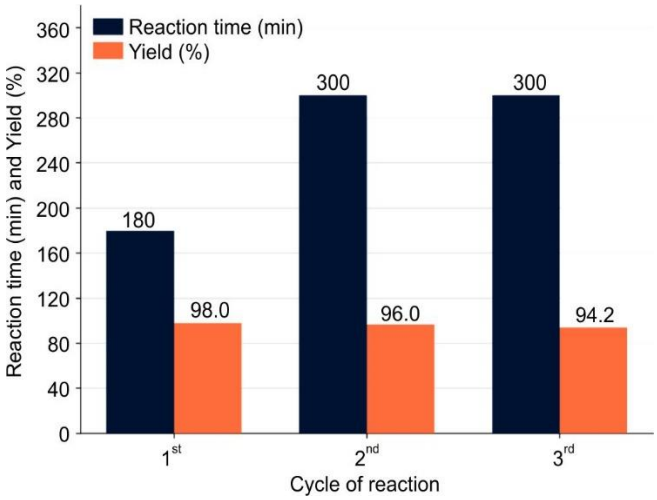

Fig. 8. Reusability of calcined *Azolla pinnata* catalyst. Reaction conditions: catalyst loading = 20 wt.%, oil to methanol molar ratio = 1:10, reaction temperature = 32 ºC

derived heterogeneous catalysts, including banana trunk ash, where the biodiesel yield decreased from 96% to 91% after three cycles [10]. Likewise, Suryaputra *et al.* [17] reported that a waste capiz shell catalyst remained reusable up to three cycles despite a reduction in activity, while Hu *et al.* [10] observed only a 10% decrease in catalytic activity for a calcined freshwater mussel shell catalyst after 12th reaction cycles. These results demonstrate the good stability and reusability of the *A. pinnata* biochar catalyst for biodiesel production.

Leaching of the catalyst: EDX and PXRD analyses of the reused catalyst were performed to investigate the leaching of active species during repeated transesterification cycles. EDX analysis (Table-1) showed a progressive decrease in the wt.% of Na, K and Cl from 9.75, 20.12 and 19.48, respectively, in the fresh catalyst to 5.74, 7.31 and 0.24 after the third reuse, indicating partial loss of these inorganic species. This observation was validated by the PXRD patterns, which showed the disappearance of the characteristic diffraction peaks of KCl and NaCl after repeated use. The reduction of these phases suggests partial leaching or transformation of the active components during transesterification, which likely contributes to the slight decline in catalytic activity. Nevertheless, despite the gradual loss of Na-, K- and Cl-containing species, the catalyst retained high catalytic efficiency over three reaction cycles, demonstrating its good stability and reusability for biodiesel production.

The comprehensive characterisation of the *A. pinnata* biochar catalyst indicates that calcination at 500 ºC produces a mineral-rich heterogeneous catalyst containing abundant alkali and alkaline earth species. PXRD analysis identified KCl, NaCl and SiO_2 as the predominant crystalline phases, together with moderate amounts of CaO, MgO, $CaCO_3$ and $K_3Na(SO_4)_2$. EDX analysis further confirmed that K, Na, Cl, Si, C and O are the major elemental constituents, while Ca and Mg are present in moderate concentrations and P, Fe, Mn and N occur only in trace amounts. The decrease in the concentrations of K, Na and Cl after repeated catalytic cycles, together with the disappearance of the corresponding PXRD peaks, suggests that these species contribute significantly to the catalytic activity.

Although the BET surface area of the calcined catalyst (11 m^2/g) is modest compared with many conventional heterogeneous catalysts, catalytic activity is not governed solely by surface area. In biomass-derived catalysts, the nature, accessibility and strength of the active sites often play a more key role than the total surface area. The presence of basic oxides such as CaO and MgO is expected to provide Lewis basic O^{2-} surface sites that promote methoxide ion formation, thereby facilitating the transesterification reaction. In addition, the alkali metal species may modify the electronic properties and basicity of the catalyst surface, enhancing reactant adsorption and catalytic performance. Similar synergistic effects of alkali and alkaline earth species have been reported for biomass-derived catalysts used in transesterification reactions [18].

Despite exhibiting excellent catalytic performance, the catalyst showed a gradual decline in activity upon reuse. EDX and PXRD analyses demonstrated partial leaching of Na-, K- and Cl-containing phases during successive reaction cycles, which is consistent with the observed decrease in biodiesel yield. The loss of these active inorganic species indicates that they participate directly in the catalytic process. Consequently, while the catalyst predominantly functions as a heterogeneous catalyst, the partial leaching of alkali species suggests that a limited homogeneous contribution during the reaction cannot be completely excluded. Nevertheless, the catalyst maintained high biodiesel yields after three consecutive cycles, demonstrating good stability and promising reusability for sustainable biodiesel production.

Comparative studies: Optimisation of the transesterification parameters established that the optimum conditions for converting tamarind seed oil to biodiesel were a methanol-to-oil ratio of 10:1, 20 wt.% catalyst loading, 3 h reaction time, and room temperature, affording a maximum biodiesel yield of 98%. A comparison of the present catalyst with previously reported waste biomass-derived heterogeneous catalysts is shown in Table-5. The *A. pinnata* biochar catalyst exhibited excellent catalytic performance, which can be attributed to the synergistic contribution of its alkali and alkaline earth components. Although catalysts with both lower and higher BET surface areas have been reported [13,19,20,26-28], the present catalyst achieved a high biodiesel yield, indicating that catalytic activity is governed primarily by the nature and strength of the active sites rather than surface area alone. The transesterification conditions and biodiesel yield of the reported waste biomass-derived catalysts are showed in Table-5.

Conclusion

Tamarind seeds are an abundant byproduct of the tamarind pulp industry and are largely underutilised despite

TABLE-5
Azolla pinnata CATALYST PERFORMANCE IN COMPARISON TO PREVIOUSLY REPORTED WASTE BIOMASS HETEROGENEOUS BASE CATALYSTS FOR BIODIESEL SYNTHESIS AND THE EFFECTS OF REACTION VARIABLES ON THE YIELD OF BIODIESEL

Waste biomass catalyst source	C_T (ºC)	C_t (h)	C_{SA} ($m^2 g^{-1}$)	Reusability (R_{cyc})	Biodiesel feedstock	MTOR	Catalyst loading (wt.%)	Time (h)	Temp. (ºC)	Yield (%)	Ref.
Azolla pinnata	500	3	11	3	Tamarind seed oil	10:1	20.0	3.0	32	98.00	This work
Waste eggshell	800	2	–	13	Soybean oil	9:1	3.0	3.0	65	95.00	[5]
Acid treated quail eggshells	800	2	14	5	Palm olein oil	12:1	0.5	2.0	65	90.00	[11]
Waste mud crab (*Scylla serrata*) shell	700	2	13	11	Palm olein	0.5:1	5.0	2.5	65	96.00	[12]
Waste obtuse horn shell	800	3	0.07	3	Palm oil	12:1	5.0	6.0	65	86.70	[13]
Waste capiz (*Amusium cristatum*) shell	900	2	–	3	Palm oil	8:1	3.0	6.0	60	93.00	[17]
Waste shells of egg, golden apple snail and meretrix venus	800	2-4	1.1, 0.9 and 0.5	–	Palm olein oil	12:1	10.0	2.0	60	90.00	[19]
Industrial waste fly ash and chicken egg shell	1000	2	0.7	16	Soybean oil	6.9:1	30.0	5.0	70	96.50	[20]
A mixture of calcined waste mud crab shells and cockleshells in a 1:1 mass ratio	900	2	12.8	–	Waste cooking oil	13:1	5.0	3.0	65	98.00	[21]
White bivalve clam shells	900	4	–	–	Waste frying oil	18:1	8.0	3.0	65	95.80	[22]
Waste mussel shell	1050	2	–	5	Soybean oil	24:1	12.0	8.0	60	94.10	[23]
Calcined scallop waste shell	1000	4	74.9	–	Palm oil	9:1	10.0	3.0	65	95.40	[24]
Palm kernel shell ash	800	2	13.7	–	Sunflower oil	9:1	5.0	0.5	60	99.00	[25]
Angel wing shell (*Cyrtopleura costata*)	900	2	3.8	3	Microalgae (*Nannochloropsis oculata)* oil	150:1	9.0	1.0	65	84.10	[26]
Calcined scallop shell	1000	2	7.3	3	Waste cooking oil	6:1	5.0	2.0	65	86.00	[27]
Brassica nigra (black mustard)	550	2	7.3	3	Soybean oil	12:1	7.0	0.4	65	98.00	[28]
Modified eggshell-derived CaO catalysts	800	4	23.3	3	Jatropha oil	27.6:1	4.7	1.4	65	99.71	[29]

C_T = calcination temperature, C_t = calcination time, C_{SA} = catalyst surface area, R_{cyc} = reaction cycles, MTOR = methanol to oil ratio.

containing appreciable quantities of oil. Since the seeds are unsuitable for direct consumption due to the presence of tannins and other colouring compounds, the extraction of tamarind kernel oil from waste tamarind kernel powder (TKP) provides a sustainable feedstock for biodiesel production, adding value to an agricultural waste stream. The utilisation of *A. pinnata*, an invasive aquatic weed, as a catalyst precursor further enhances the sustainability of the process. Under the optimised conditions (methanol-to-oil ratio of 10:1, catalyst loading of 20 wt.% and reaction time of 3 h), the catalyst afforded a biodiesel yield of 98%. The catalyst was readily recovered and reused, producing 96.6% biodiesel after the first reuse and 94.2% after the second reuse, with only a modest increase in reaction time. These results demonstrate the excellent catalytic activity, stability and reusability of the catalyst. Future studies will focus on identifying the catalytically active sites and elucidating the reaction mechanism to further improve catalyst performance and long-term stability.

ACKNOWLEDGEMENTS

The authors acknowledge the Department of Chemistry, Gauhati University for allowing us to investigate sample through PXRD, TGA, BET, FESEM, EDX, ^{1}H NMR spectral analysis.

CONFLICT OF INTEREST

The authors declare that there is no conflict of interests regarding the publication of this article.

DECLARATION OF AI-ASSISTED TECHNOLOGIES

During the preparation of this manuscript, the authors used an AI-assisted tool(s) to improve the language and no data, results or scientific conclusions were generated by AI. All analyses, interpretations and conclusions are the authors' own. The authors reviewed and edited the content and take full responsibility for the published work.

REFERENCES

1. A. Jess, *Energy Policy*, **38**, 4663 (2010); https://doi.org/10.1016/j.enpol.2010.04.026
2. Y. He, S. Wang and K.K. Lai, *Energy Econ.*, **32**, 868 (2010); https://doi.org/10.1016/j.eneco.2009.12.005
3. B. Abdullah, S.A.F. Syed Muhammad, Z. Shokravi, S. Ismail, K.A. Kassim, A.N. Mahmood and M.M.A. Aziz, *Renew. Sustain. Energy Rev.*, **107**, 37 (2019); https://doi.org/10.1016/j.rser.2019.02.018
4. Y.S. Rao and K.M. Mathew, *Tamarind*, 2, 512 (2012); https://doi.org/10.1533/9780857095688.512
5. Z. Wei, C. Xu and B. Li, *Bioresour. Technol.*, **100**, 2883 (2009); https://doi.org/10.1016/j.biortech.2008.12.039
6. N. Nakatani, H. Takamori, K. Takeda and H. Sakugawa, *Bioresour. Technol.*, **100**, 1510 (2009); https://doi.org/10.1016/j.biortech.2008.09.007
7. T.A. Lumpkin and D.L. Plucknett, *Econ. Bot.*, **34**, 111 (1980); https://doi.org/10.1007/BF02858627
8. V. Vadery, B.N. Narayanan, R.M. Ramakrishnan, S. Sugunan, S.K. Cherikkallinmel, D.P. Narayanan and S. Sasidharan, *Energy*, **70**, 588 (2014); https://doi.org/10.1016/j.energy.2014.04.045
9. J. Wang, S. Xing, Y. Huang, P. Fan, J. Fu, G. Yang, L. Yang and P. Lv, *Appl. Energy*, **190**, 703 (2017); https://doi.org/10.1016/j.apenergy.2017.01.004
10. S. Hu, Y. Wang and H. Han, *Biomass Bioenergy*, **35**, 3627 (2011); https://doi.org/10.1016/j.biombioe.2011.05.009
11. Y.B. Cho and G. Seo, *Bioresour. Technol.*, **101**, 8515 (2010); https://doi.org/10.1016/j.biortech.2010.06.082
12. P.L. Boey, G.P. Maniam and S.A. Hamid, *J. Oleo Sci.*, **58**, 499 (2009); https://doi.org/10.5650/jos.58.499
13. S.L. Lee, Y.C. Wong, Y.P. Tan and S.Y. Yew, *Energy Convers. Manage.*, **93**, 282 (2015); https://doi.org/10.1016/j.enconman.2014.12.067

14. T. Dong, D. Gao, C. Miao, X. Yu, C. Degan, M. Garcia-Pérez, B. Rasco, S.S. Sablani and S. Chen, *Energy Convers. Manage.*, **105**, 1389 (2015); https://doi.org/10.1016/j.enconman.2015.06.072
15. A.E. Atabani, A.S. Silitonga, H.C. Ong, T.M.I. Mahlia, H.H. Masjuki, I.A. Badruddin and H. Fayaz, *Renew. Sustain. Energy Rev.*, **18**, 211 (2013); https://doi.org/10.1016/j.rser.2012.10.013
16. G. Pathak, D. Das, K. Rajkumari and S.L. Rokhum, *Green Chem.*, **20**, 2365 (2018); https://doi.org/10.1039/C8GC00071A
17. W. Suryaputra, I. Winata, N. Indraswati and S. Ismadji, *Renew. Energy*, **50**, 795 (2013); https://doi.org/10.1016/j.renene.2012.08.060
18. M. Safar, B.-J. Lin, W.-H. Chen, D. Langauer, J.-S. Chang, H. Raclavska, A. Pétrissans, P. Rousset and M. Pétrissans, *Appl. Energy*, **235**, 346 (2019); https://doi.org/10.1016/j.apenergy.2018.10.065
19. N. Viriya-empikul, P. Krasae, B. Puttasawat, B. Yoosuk, N. Chollacoop and K. Faungnawakij, *Bioresour. Technol.*, **101**, 3765 (2010); https://doi.org/10.1016/j.biortech.2009.12.079
20. R. Chakraborty, S. Bepari and A. Banerjee, *Chem. Eng. J.*, **165**, 798 (2010); https://doi.org/10.1016/j.cej.2010.10.019
21. P.L. Boey, S. Ganesan, G.P. Maniam and M. Khairuddean, *Catal. Today*, **190**, 117 (2012); https://doi.org/10.1016/j.cattod.2011.11.027
22. N. Girish, S.P. Niju, K.M. Meera Sheriffa Begum and N. Anantharaman, *Fuel*, **111**, 653 (2013); https://doi.org/10.1016/j.fuel.2013.03.069
23. R. Rezaei, M. Mohadesi and G.R. Moradi, *Fuel*, **109**, 534 (2013); https://doi.org/10.1016/j.fuel.2013.03.004
24. A. Buasri, P. Worawanitchaphong, S. Trongyong and V. Loryuenyong, *APCBEE Procedia*, **8**, 216 (2014); https://doi.org/10.1016/j.apcbee.2014.03.030
25. M.D. Kostić, A. Bazargan, O.S. Stamenković, V.B. Veljković and G. McKay, *Fuel*, **163**, 304 (2016); https://doi.org/10.1016/j.fuel.2015.09.042
26. O. Nur Syazwani, U. Rashid and Y.H. Taufiq Yap, *Energy Convers. Manage.*, **101**, 749 (2015); https://doi.org/10.1016/j.enconman.2015.05.075
27. S. Sirisomboonchai, M. Abuduwayiti, G. Guan, C. Samart, S. Abliz, X. Hao, K. Kusakabe and A. Abudula, *Energy Convers. Manage.*, **95**, 242 (2015); https://doi.org/10.1016/j.enconman.2015.02.044
28. B. Nath, B. Das, P. Kalita and S. Basumatary, *J. Clean. Prod.*, **239**, 118112 (2019); https://doi.org/10.1016/j.jclepro.2019.118112
29. S. Palitsakun, K. Koonkuer, B. Topool, A. Seubsai and K. Sudsakorn, *Catal. Commun.*, **149**, 106233 (2021); https://doi.org/10.1016/j.catcom.2020.106233
30. G.M. Wagner, *Bot. Rev.*, **63**, 1 (1997); https://doi.org/10.1007/BF02857915